

# FPGA Realization of Inverse Kinematics for Biped Robot Based on CORDIC

C.C. Wong and C.C. Liu

A FPGA realization structure based on CORDIC is proposed to implement inverse kinematics for biped robot. First, the angle equations of inverse kinematics for biped robot are described. Based on these equations represented by the inverse tangent function, a FPGA structure based on two CORDIC operators of Circular Vectoring (CV) and Hyperbolic Vectoring (HV) is proposed and implemented on a FPGA chip. Finally, the comparison of the proposed FPGA realization and the software realization to calculate these angle equations are presented to illustrate the effectiveness of the proposed structure.

**Introduction:** Researches related to the control of biped robots have made a lot. However, the real-time control of biped robot still remains a challenge for such a high-order highly-coupled nonlinear dynamical system. For example, the system clock of the embedded system for the real-time control of the small-sized biped robot [1] is limited, some efficient methods are needed to accelerate the calculation speed. COordinate Rotation DIGital Computer (CORDIC) algorithm provides a simplified method for calculating the trigonometric and square-root. And it reduces computational time and power consumption. Some CORDIC designs have been implemented on a Field Programmable Gate Array (FPGA) chip [2-3], such as mobile robot exploration [4] and kinematics control for manipulator [5]. FPGA-based system is useful because it can reduce development time, reprogrammed on the fly, and operate faster than microprocessor [6]. However, there is no research related to the FPGA realization of inverse kinematics for biped robot based on CORDIC. Thus a CORDIC-based realization method for the computation of inverse kinematics for biped robot is proposed in this letter. The computation time can be considerably reduced by the proposed method so that it can be applied to improve the performance of real-time control of biped robot.

**Inverse Kinematics Equations for Biped Robot:** The link coordinate system of the biped robot is shown in Fig. 1, where  $l_1$  and  $l_2$  ( $l_3$  and  $l_4$ ) respectively denotes the length of thigh and shank of the right (left) foot. When the desired positions  $P_{R\_Hip} = (x_{RH}, y_{RH}, z_{RH})$  ( $P_{L\_Hip} = (x_{LH}, y_{LH}, z_{LH})$ ) and  $P_{R\_Foot} = (x_{RF}, y_{RF}, z_{RF})$  ( $P_{L\_Foot} = (x_{LF}, y_{LF}, z_{LF})$ ) of the right (left) hip and foot are given, the values of  $(x_R, y_R, z_R)$  and  $(x_L, y_L, z_L)$  described in Fig.1 can be obtained by

$$(x_R, y_R, z_R) = (x_{RH} - x_{RF}, y_{RH} - y_{RF}, z_{RH} - z_{RF}) \quad (1)$$

$$(x_L, y_L, z_L) = (x_{LH} - x_{LF}, y_{LH} - y_{LF}, z_{LH} - z_{LF}) \quad (2)$$

Then the angle equations of the inverse kinematics for the biped robot from  $(x_R, y_R, z_R; x_L, y_L, z_L; l_1, l_2, l_3, l_4)$  to  $(\theta_1, \theta_2, \dots, \theta_{10})$  can be obtained as follows:

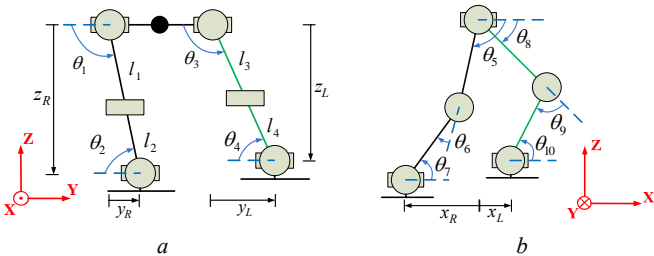


**Fig. 1** The link coordinate system of the biped robot.

a The schematic of y and z magnitudes in right foot and left foot  
b The schematic of x magnitudes in the right foot and left foot

In Fig. 1(a), we can obtain the following four equations:

$$\theta_1 = \tan^{-1}(-z_R/y_R) \quad (3)$$

$$\theta_2 = \pi - \theta_1 \quad (4)$$

$$\theta_3 = \tan^{-1}(-z_L/y_L) \quad (5)$$

$$\theta_4 = \pi - \theta_3 \quad (6)$$

where  $\theta_1$  and  $\theta_2$  ( $\theta_3$  and  $\theta_4$ ) denote the hip and ankle angle of the right (left) foot, respectively. We can see that  $\theta_1$  and  $\theta_2$  ( $\theta_3$  and  $\theta_4$ ) are generated by the magnitudes of  $y_R$  and  $z_R$  ( $y_L$  and  $z_L$ ).

In Fig. 1(b), we can obtain the following equations:

$$\theta_5 = 2 \tan^{-1} \left( \frac{l_R^2 + l_1^2 - l_2^2}{2l_1 l_R + \sqrt{(2l_1 l_R)^2 - (l_R^2 + l_1^2 - l_2^2)^2}} \right) - 2 \tan^{-1} \left( \frac{x_R}{l_R + (-z_R)} \right) \quad (7)$$

$$\theta_6 = 2 \tan^{-1} \left( \frac{\sqrt{(2l_1 l_2)^2 - (l_R^2 + l_1^2 - l_2^2)^2}}{2l_1 l_2 + (l_R^2 + l_1^2 - l_2^2)} \right) \quad (8)$$

$$\theta_7 = \pi - \theta_5 - \theta_6 \quad (9)$$

$$\theta_8 = 2 \tan^{-1} \left( \frac{l_L^2 + l_3^2 - l_4^2}{2l_3 l_L + \sqrt{(2l_3 l_L)^2 - (l_L^2 + l_3^2 - l_4^2)^2}} \right) - 2 \tan^{-1} \left( \frac{x_L}{l_L + (-z_L)} \right) \quad (10)$$

$$\theta_9 = 2 \tan^{-1} \left( \frac{\sqrt{(2l_3 l_4)^2 - (l_L^2 + l_3^2 - l_4^2)^2}}{2l_3 l_4 + (l_L^2 + l_3^2 - l_4^2)} \right) \quad (11)$$

$$\theta_{10} = \pi - \theta_8 - \theta_9 \quad (12)$$

$$l_R = \sqrt{x_R^2 + (-z_R)^2} \quad (13)$$

$$l_L = \sqrt{x_L^2 + (-z_L)^2} \quad (14)$$

where  $\theta_5, \theta_6,$  and  $\theta_7$  ( $\theta_8, \theta_9,$  and  $\theta_{10}$ ) denote the hip, knee, and ankle angle of the right (left) foot, respectively. We can see that  $\theta_5 \sim \theta_7$  ( $\theta_8 \sim \theta_{10}$ ) are generated by the magnitudes of  $x_R, z_R, l_1,$  and  $l_2$  ( $x_L, z_L, l_3,$  and  $l_4$ ).

Note that these angle equations are modified to be represented by the inverse tangent function so that the CORDIC algorithm can be effectively implemented in FPGA.

**FPGA Realization of Inverse Kinematics of Biped Robot:** In this letter, two CORDIC operators shown in Table 1 are implemented and used in the FPGA realization. Based on these angle equations described in Equations (3)~(12), the system block of FPGA realization of inverse kinematics for the biped robot can be described by Fig. 2. Four Function Modules (FM) based on CORDIC operators are described as follows:

**Table 1:** Symbol and function of two CORDIC operators.

Circular Vectoring (CV) Operator	Hyperbolic Vectoring (HV) Operator
$x_0 \rightarrow$ $y_0 \rightarrow$ $z_0 = 0 \rightarrow$	$x_0 \rightarrow$ $y_0 \rightarrow$ $z_0 = 0 \rightarrow$
$x_n = \sqrt{x_0^2 + y_0^2}$ $y_n = 0$ $z_n = \tan^{-1}(y_0/x_0)$	$x_n = \sqrt{x_0^2 - y_0^2}$ $y_n = 0$ $z_n = \tanh^{-1}(y_0/x_0)$

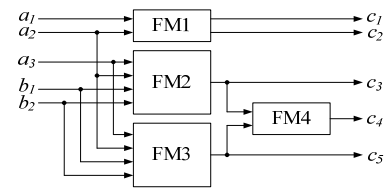


**Fig. 2** System block of FPGA realization of inverse kinematics.

Based on Equations (3) and (4), the FPGA structure of FM 1 described in Fig. 3 based on CORDIC operators can be used to obtain  $c_1 = \theta_1$  and  $c_2 = \theta_2$ , where the inputs are  $a_1 = y_R$  and  $a_2 = -z_R$ . Similarly,  $\theta_3$  and  $\theta_4$  can be obtained when the inputs of FM 1 are  $a_1 = y_L$  and  $a_2 = -z_L$ .

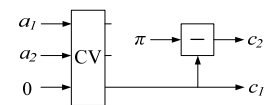


**Fig. 3** FPGA structure of FM 1 used to calculate  $\theta_1$  and  $\theta_2$  ( $\theta_3$  and  $\theta_4$ ).

Based on Equation (7), the FPGA structure of FM 2 described in Fig. 4 based on CORDIC operators can be used to obtain  $c_3 = \theta_5$ , where the inputs are  $a_2 = -z_R, a_3 = x_R, b_1 = l_1,$  and  $b_2 = l_2$ . Similarly,  $\theta_8$  can be obtained when the inputs of FM 2 are  $a_2 = -z_L, a_3 = x_L, b_1 = l_3,$  and  $b_2 = l_4$ .

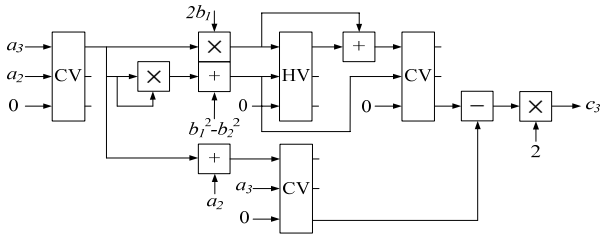


**Fig. 4** FPGA structure of FM 2 used to calculate  $\theta_5$  ( $\theta_8$ ).

Based on Equation (8), the FPGA structure of FM 3 described in Fig. 5 based on CORDIC operators can be used to obtain  $c_5=\theta_6$ , where the inputs are  $a_2=-z_R$ ,  $a_3=x_R$ ,  $b_1=l_1$ , and  $b_2=l_2$ . Similarly,  $\theta_9$  can be obtained when the inputs of FM 3 are  $a_2=-z_L$ ,  $a_3=x_L$ ,  $b_1=l_3$ , and  $b_2=l_4$ .

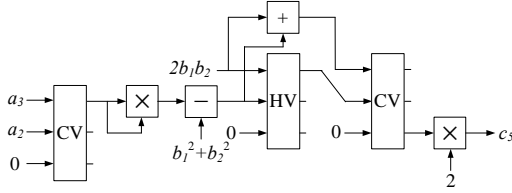


**Fig. 5** FPGA structure of FM 3 used to calculate  $\theta_6$  ( $\theta_9$ ).

Based on Equation (9), the FPGA structure of FM 4 described in Fig. 6 can be used to obtain  $c_4=\theta_7$ , where the inputs are  $c_3=\theta_3$  and  $c_5=\theta_6$  are inputs. Similarly,  $\theta_{10}$  can be obtained when the inputs of FM 4 are  $c_3=\theta_8$  and  $c_5=\theta_9$ .

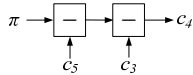


**Fig. 6** FPGA structure of FM 4 used to calculate  $\theta_7$  ( $\theta_{10}$ ).

**Results and Conclusion:** To illustrate the effectiveness of the proposed CORDIC-based structure, it is realized by Verilog HDL (Hardware Description Language) and implemented in a DE II development board. In this board, the adopt FPGA chip is Altera Cyclone-IV on Quartus II platform. To test the accuracy of the proposed method, some computation results of the software and the proposed FPGA (hardware) realization to calculate the angles of inverse kinematic for biped robot are considered. From the experimental results, the maximum error between the software and the proposed hardware realization to calculate  $\theta_1$  ( $\theta_3$ ),  $\theta_2$  ( $\theta_4$ ),  $\theta_5$  ( $\theta_8$ ),  $\theta_6$  ( $\theta_9$ ), and  $\theta_7$  ( $\theta_{10}$ ) are 0.00053 (0.00061), 0.00087 (0.00088), -0.01816 (-0.02031), 0.038 (0.038), and -0.02675 (-0.02755), respectively. For example, the computation results of  $\theta_6$  are shown in Fig. 7, where a complete walking process including starting, steady and ending is described. These errors are accepted for the real-time control of biped robot. To test the calculation speed of the proposed method, the execution number of clocks to calculate  $\theta_1$  ( $\theta_3$ ),  $\theta_2$  ( $\theta_4$ ),  $\theta_5$  ( $\theta_8$ ),  $\theta_6$  ( $\theta_9$ ), and  $\theta_7$  ( $\theta_{10}$ ) by the proposed FPGA realization are 12, 13, 43, 42, and 44, respectively. The execution time ( $\mu\text{s}$ ) of  $\theta_1\sim\theta_{10}$  by the software and hardware methods are shown in Table 2, where a 32-bit soft-cored Nios II CPU are embedded on the FPGA chip to run the software program and the system clock is 100 MHz. Note that the calculation by the software program is sequential, but the calculation by the hardware is parallel. We can see that the processing speed of the proposed hardware-implemented method is approximately 7595 times faster than that of its software counterpart run in the soft-cored Nios II CPU. Therefore, the computation time for the inverse kinematics computations for biped robot is considerably reduced by the proposed CORDIC-based FPGA realization method. It can be used to improve the real-time control of biped robot.

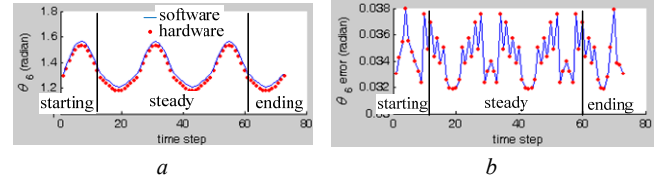


**Fig. 7** Computation results of the software and hardware realization.  
a Computation results of  $\theta_6$   
b Computation errors of  $\theta_6$

**Table 2:** Comparison of the execution time ( $\mu\text{s}$ ) of  $\theta_1\sim\theta_{10}$  by the software and hardware realization.

Angle	$\theta_1$	$\theta_2$	$\theta_3$	$\theta_4$	$\theta_5$	$\theta_6$	$\theta_7$	$\theta_8$	$\theta_9$	$\theta_{10}$	$\theta_1\sim\theta_{10}$
Software	277	318	277	318	857	522	1331	857	522	1331	3342
Hardware	0.12	0.13	0.12	0.13	0.43	0.42	0.44	0.43	0.42	0.44	0.44

**Acknowledgments:** This research was supported in part by the National Science Council (NSC) under contract NSC 101-2221-E-032-020.

C.C. Wong and C.C. Liu (Department of Electrical Engineering, Tamkang University, Tamsui, New Taipei City 25137, Taiwan)  
E-mail: wong@ee.tku.edu.tw

## References

- Wong, C.C., Cheng, C.T., Huang, K.H., and Yang, Y.T.: 'Fuzzy control of humanoid robot for obstacle avoidance', *International Journal of Fuzzy Systems*, 2008, **10**, (1), pp.261-270
- Melnikoff, S.J., and Quigley, S.F.: 'Implementing log-add algorithm in hardware', *Electronics Letters*, 2003, **39**, (12), pp. 939-941
- Sansaloni, T., Pe rez-Pascual, A., and Valls, J.: 'Area-efficient FPGA-based FFT processor', *Electronics Letters*, 2003, **39**, (19), pp. 1369-1370
- Vachhani, L., Sridharan, K., and Meher, P.K.: 'Efficient FPGA realization of CORDIC with application to robotic exploration', *IEEE Transactions on Industrial Electronics*, 2009, **56**, (12), pp. 4915-4929
- Zheng, Y., Liu, J., and Kan, J.: 'An optimal kinematics calculation method for a multi-DOF manipulator', *Przeglad Elektrotechniczny*, 2012, **88**, (7B), pp. 320-323
- Wong, C.C., and Lin, Y.H.: 'Design and implementation of GA-based fuzzy system on FPGA chip', *Cybernetics and Systems: An International Journal*, 2008, **39**, (1), pp.79-107